

ANALYSIS OF SURFACE HOAR GROWTH UNDER SIMULATED METEOROLOGICAL CONDITIONS

Brad Stanton*, Daniel Miller, Edward Adams
Montana State University Bozeman, MT

ABSTRACT: Surface hoar, essentially frozen dew, is known to form on cold, clear nights when radiant energy loss to the sky drives the surface temperature of the snow below the frost point temperature. As the surface temperature drops, the air above becomes supersaturated with respect to the snow causing the deposition of a faceted layer known as surface hoar. Few studies have attempted to grow surface hoar in a lab setting and none have replicated the radiant cooling process. In an environmental chamber at Montana State University's Subzero Science and Research Facility, surface hoar was grown using a cold ceiling to simulate long wave radiation loss to a clear sky. Air and snow temperature, wind speed, and supersaturation were carefully controlled in the lab. A time history of resulting laboratory crystal development was documented before, during, and after growth using both visible photography and 3D x-ray computed tomography (CT). Consistent with atmospheric crystal growth, results show surface hoar crystal habit varies with temperature. At snow surface temperatures of approximately -5°C and -30°C , c-axis dominant growth occurred, while at snow surface temperatures of approximately -13°C , a-axis dominant growth occurred. Additionally, specific surface area from CT scans indicated larger values for plate growth than for needles.

1. INTRODUCTION

The effect of temperature and supersaturation on crystal development has been carefully examined in several studies (i.e. Hallett and Mason, 1958; Kobayashi, 1961; Nakaya, 1954). Nakaya (1954) nucleated individual crystals on rabbit hair and found air temperature was the primary factor in determining whether a-axis or c-axis growth dominated. Kobayashi (1961) confirmed this result. While some debate remains as to the exact transition temperatures, it is generally accepted that a-axis growth dominates from 0 to -4°C and from -10 to -24°C while c-axis growth dominates from -4 to -10°C and at temperatures colder than -24°C . A field study by Lang and others (1984) suggests that the crystal habit/temperature relationship also applies to crystals that form by deposition of water vapor onto an existing snow surface—essentially frozen dew or surface hoar.

Building on the above studies, in this paper a laboratory experiment accurately simulating the natural process driving surface hoar growth was designed. Equipment and procedures to control temperature, humidity, wind speed and long wave radiation interaction with the snow surface were developed. Subsequently, experiments were performed to ascertain whether the crystal habit of

surface hoar is controlled by snow surface temperature. Additionally, the evolution of specific surface area (SSA) of surface hoar growth was examined using computed tomography (CT) data.

2. METHODOLOGY

The meteorological conditions known to produce surface hoar growth, namely cold, clear nights with significant long wave radiant energy loss at the snow surface, were simulated in Montana State University's (MSU) environmental chamber, which is capable of air temperatures as low as -40°C (Figure 1).



Figure 1: A) Experimental set up. The box on the lower left provides humidity-controlled airflow through a ducting system over the snow surface in the upper right. The temperature-controlled cold ceiling above provides the long wave radiation interaction.

*Corresponding author's address: Brad Stanton, Montana State University, Dept. Civil Engineering, Bozeman, MT, USA, 59717; tel: 406-219-3898; email: bigwallbrad@hotmail.com

To mimic snow's exposure to the night sky, an insulated box (75 x 75 x 40 cm) containing an initial snow sample of rounded grains was positioned 82 cm from the lab's cold ceiling (-50°C). The resulting long wave energy loss was used to drive the snow's surface temperature to below the frost point of air blowing over the surface. Wind speed and air humidity were controlled by using 15 cm diameter fans and ducting to direct moisture-laden air from an insulated liquid water source across the snow surface.

Environmental conditions were sampled every 30 seconds during experiments by instrumentation (Figure 2) attached to an Agilent data logger.

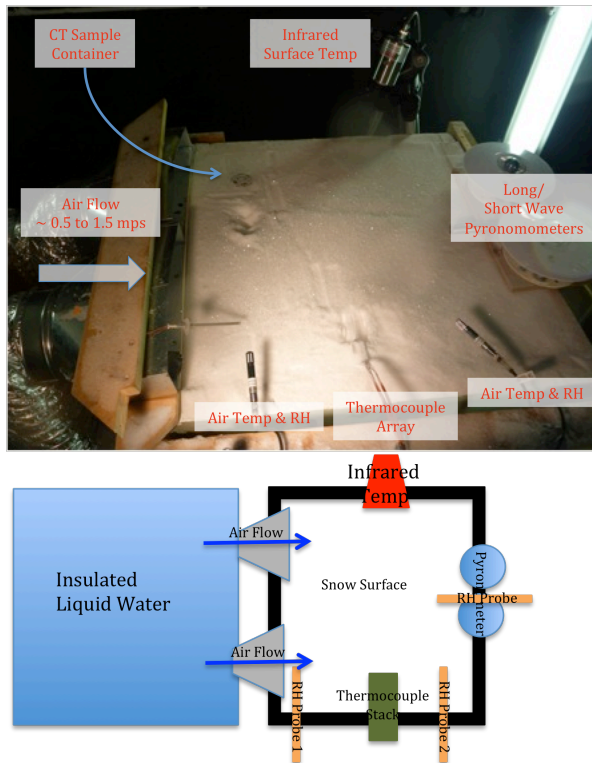


Figure 2: A) Detail of experimental set up and instrumentation. B) Functional diagram of experimental set up.

Long and short wave radiation at the snow surface were measured using a Precision Spectral Pyranometer (PSP) (0.285–2.8 μm) and a Precision Infrared Radiometer (PIR)(3.5–50 μm) from Eppley Laboratories. An Everest Interscience Model 4000-4ZL non-contact infrared sensor provided snow surface temperature measurements. Relative humidity was monitored using a Campbell Scientific, Inc. CS215 Relative

Humidity and Temperature Probe and/or a Vaisala INTERCAP Humidity and Temperature Probe HMP60. An array of thermocouples buried at 1 cm intervals captured the temperature profile within the top 7 cm of the snow pack.

Additional thermocouples monitored the air temperature 1 and 2 cm above the snow surface and at the entrance and outlet to the ducting. Cold ceiling and surrounding wall temperatures were recorded via built in thermocouples incorporated into the environmental chamber. Finally, wind speed was held constant (~0.75 to 1.5 m/s) and was measured approximately 2 to 3 times during the course of each experiment using a hand held Omega Engineering, Inc. Digital Anemometer.

To facilitate in-situ CT scans of growing surface hoar, a 34 cm³ cylindrical sample holder was buried with its top edge flush with the snow surface (Figures 2 and 3).

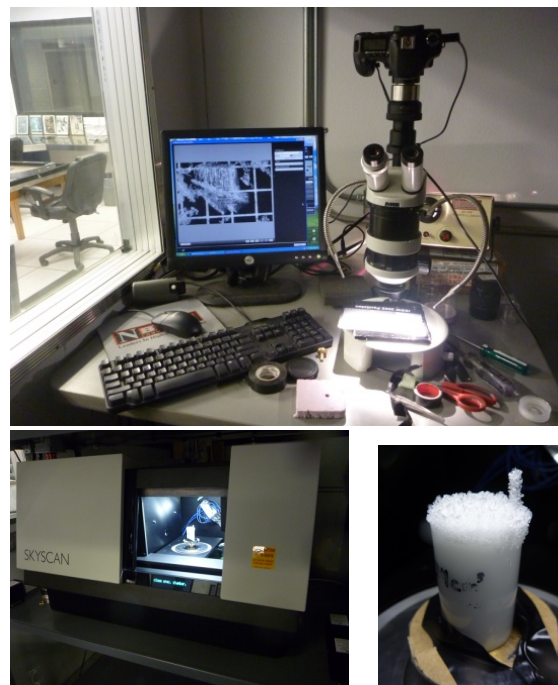


Figure 3: A) Wild optical microscope with digital imaging, B) SkyScan 1173 CT Scanner adapted for cold room use, C) 34 cm³ sample holder with surface hoar growth. The vertical rod is used for image rotational indexing.

An ASTM #8 soil sieve (mesh size: 2.36 mm) was used to both fill the sample container and sift a uniform, level layer of rounded grains onto the snow surface. Before, during, and after each experiment, the sample holder was carefully

removed, scanned using a SkyScan 1173 CT scanner, and then returned to its original position and orientation. A 0.5 mm diameter graphite cylinder was inserted into the sample container as an index reference so the CT scans could be properly oriented for comparison at different time steps (Figure 3). Simultaneously, microscopic still photographs of disaggregate grains were taken at magnifications ranging from 6x to 50x.

Two sequences of three experiments were conducted for a total of six experiments. The chamber's air temperature was varied between the three experiments and the sequence was carried out twice to demonstrate repeatability. Each experiment consisted of a 24-hour growth period, during which 3 to 5 CT scans and accompanying microscopic images were acquired. The experimental sequences are numbered 1 and 2 while the tests at specific temperatures are lettered a, b, c. During experiments 1a and 2a the chamber's air temperature was set to -30°C . During experiments 1b and 2b the chamber's air temperature was set to -13°C and, finally, during experiments 1c and 2c the chamber's air temperature was set to -5°C . These temperatures elicit dominant c-axis growth (-5°C and -30°C) and a-axis growth (-13°C) (Kobayashi, 1961). Once chamber air temperature was set, the data logger

was activated and the snow sample allowed to equilibrate with the room temperature. This initial transition in temperature generally accounts for the minimum and maximum values given in the results. Other fluctuations in surface temperature towards the end of the experiment were caused by the development of frost on the cold ceiling interfering with long wave coupling at the snow surface as well as the opening of the chamber door to sweep the frost from the ceiling. During periods of surface hoar growth, snow surface temperatures averaged $\sim 2\text{--}4^{\circ}\text{C}$ below the room's air temperature and fell within the range required for a-axis vs. c-axis growth discussed above.

3. RESULTS

Three-dimensional CT scans and select accompanying optical images are presented for each experiment in Figures 4 – 9. All CT scans were taken at a resolution of $14.8\ \mu\text{m}$. The initial image (left side) is the base surface snow that the surface hoar was allowed to develop upon. In the sequences of images, the development of surface hoar is evident in the CT and optical images. In Table 1, the test sequence is summarized with average surface temperature, dominant growth axis (as evidenced by crystal habit) and specific surface area calculated from sample CT scans.

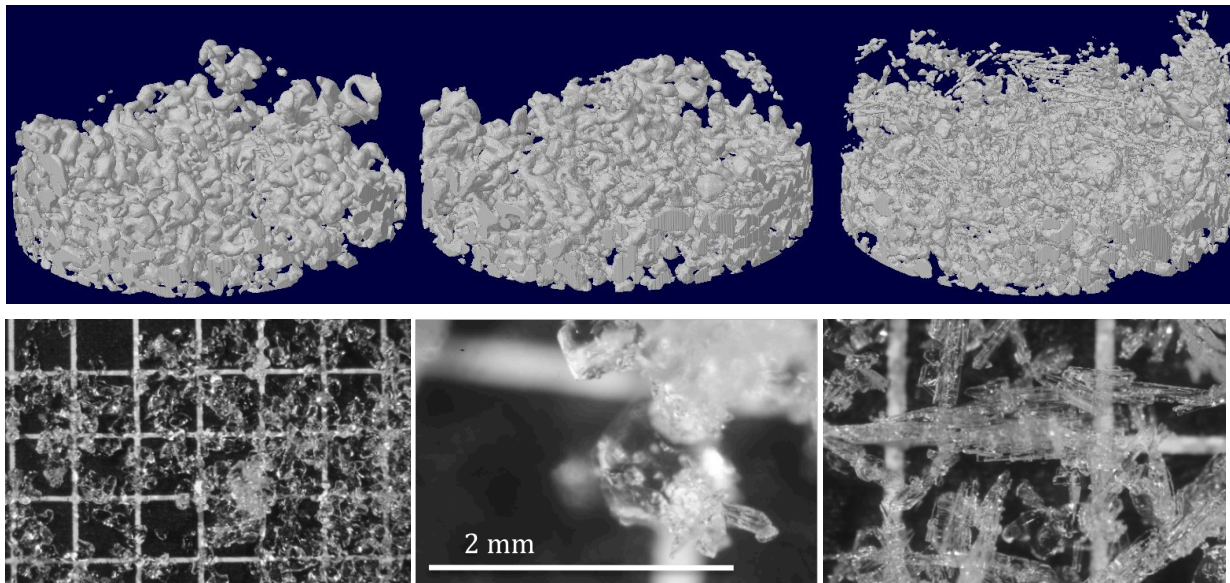


Figure 4: Test 1a. Snow surface temperature during first 7 hours of growth started at $\sim 26.8^{\circ}\text{C}$ and steadily approached a constant -31.5°C . During the final 17-hour growth period, surface temperature data failed to record; however, it is speculated the snow surface temperature remained close to -31.5°C during periods of actual surface hoar growth. CT Images at times: 0, 7, 24 (hrs) (Sample Diameter: 9.7 mm) and corresponding microscopic images (2 mm grid).

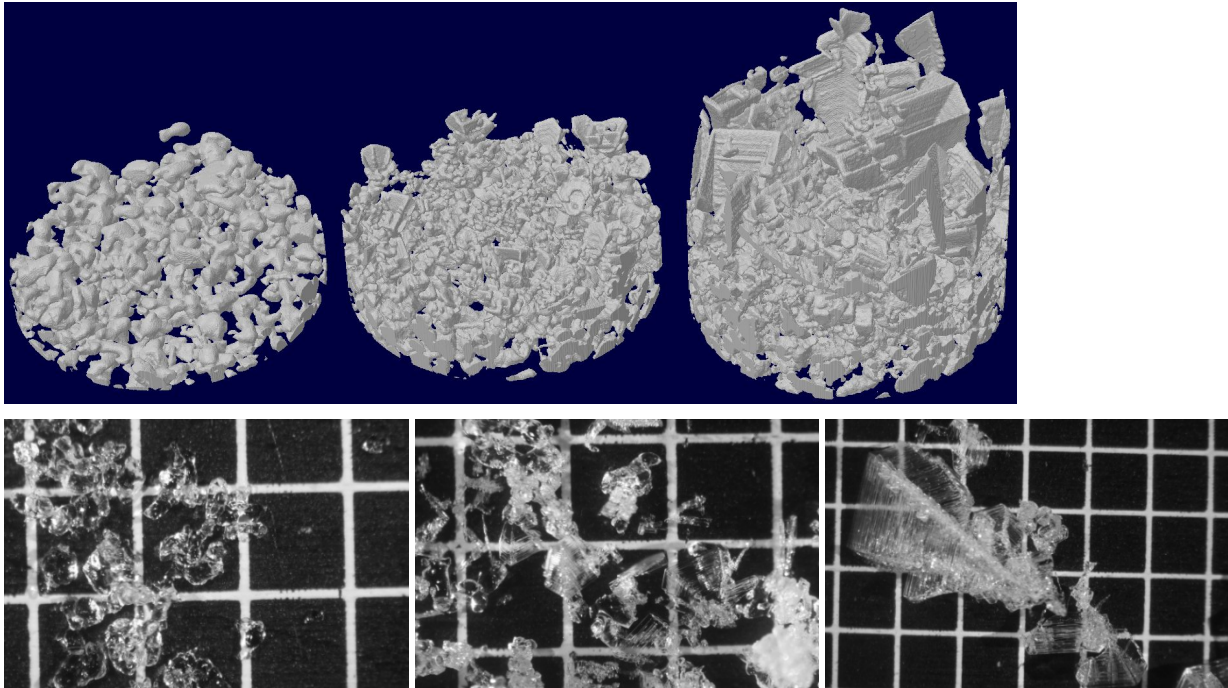


Figure 5: Test 1b. Snow Surface Temperature Range: -13.6 to -21.1°C . Mean Snow Surface Temperature: -15.5°C with a Standard Deviation of 1.9°C . CT Images at times: 0, 6.5, 22 (hrs) (Sample Diameter: 8.6 mm) and corresponding microscopic images (2 mm grid).

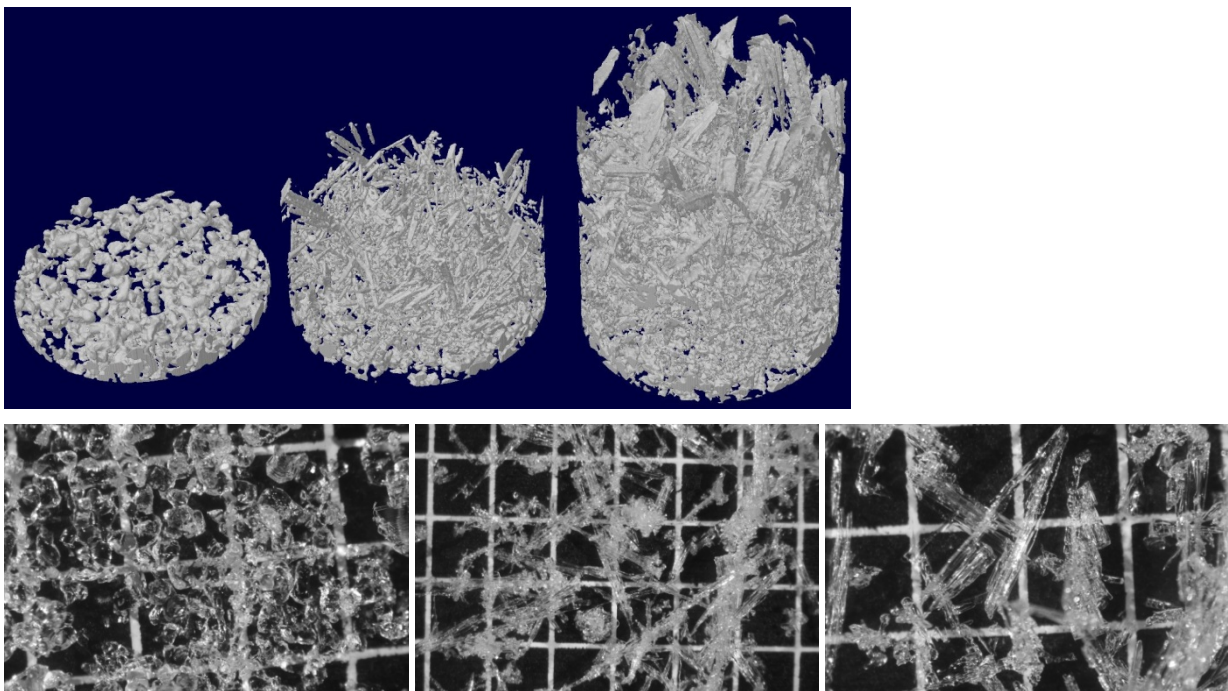


Figure 6: Test 1c. Snow Surface Temperature Range: -1.8 to -11.8°C . Mean Snow Surface Temperature: -8.3°C with a Standard Deviation of 1.0°C . CT Images at times: 0, 6.5, 22.5 (hrs) (Sample Diameter: 8.6 mm) and corresponding microscopic images (2 mm grid).

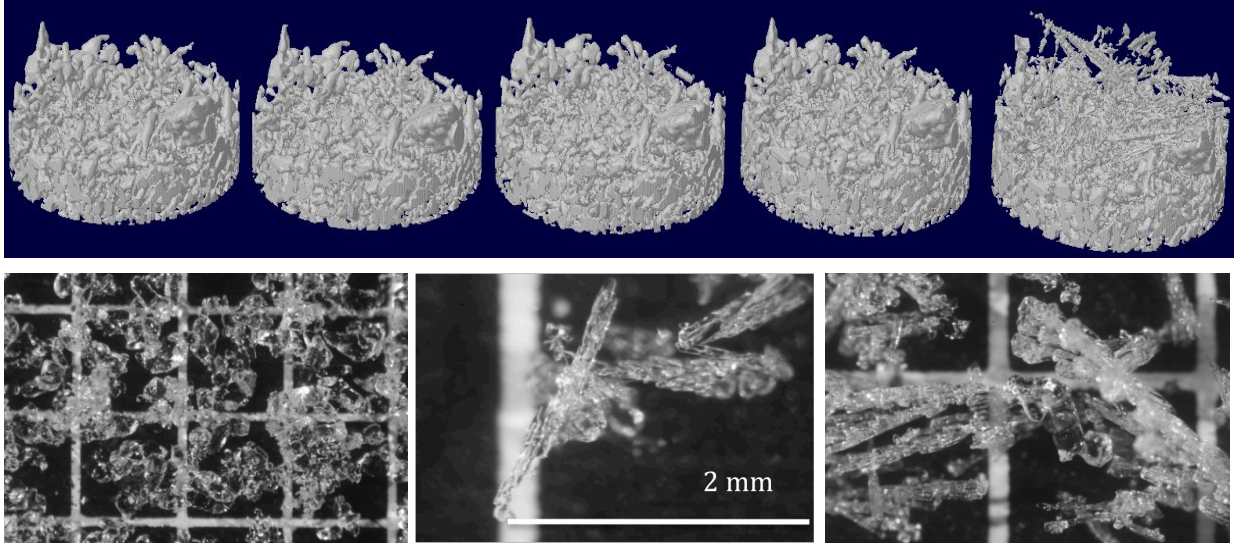


Figure 7: Test 2a. Snow Surface Temperature Range: -26.5 to -31.1°C . Mean Snow Surface Temperature: -29.7°C with a Standard Deviation of 1.2°C . CT Images at times: 0, 5, 8.5, 12.5, 25 (hrs) (Sample Diameter: 8.3 mm) and select microscopic images (2 mm grid) at time 0, 12.5, 25 (hrs). Note: during the initial 12.5 hours, the snow surface temperature dropped as the snow equilibrated with the chamber air temperature. Significant growth did not occur until the snow surface temperature dropped below this chamber air temperature, due to the long wave loss to the cold ceiling, around hour 10.

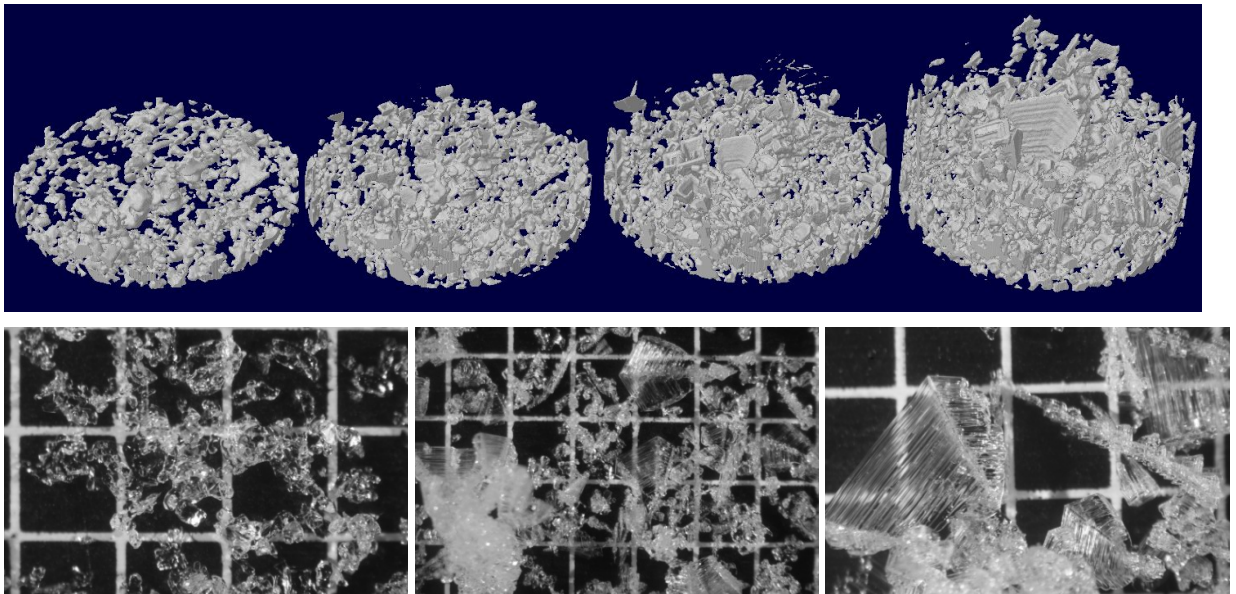


Figure 8: Test 2b. Snow Surface Temperature Range: -12.4 to -16.5°C . Mean Snow Surface Temperature: -15°C with a Standard Deviation of 0.4°C . CT Images at times: 0, 7, 12.5, 24 (hrs) (Sample Diameter: 9.8 mm) and select microscopic images (2 mm grid) at times 0, 12.5, 24 (hrs).

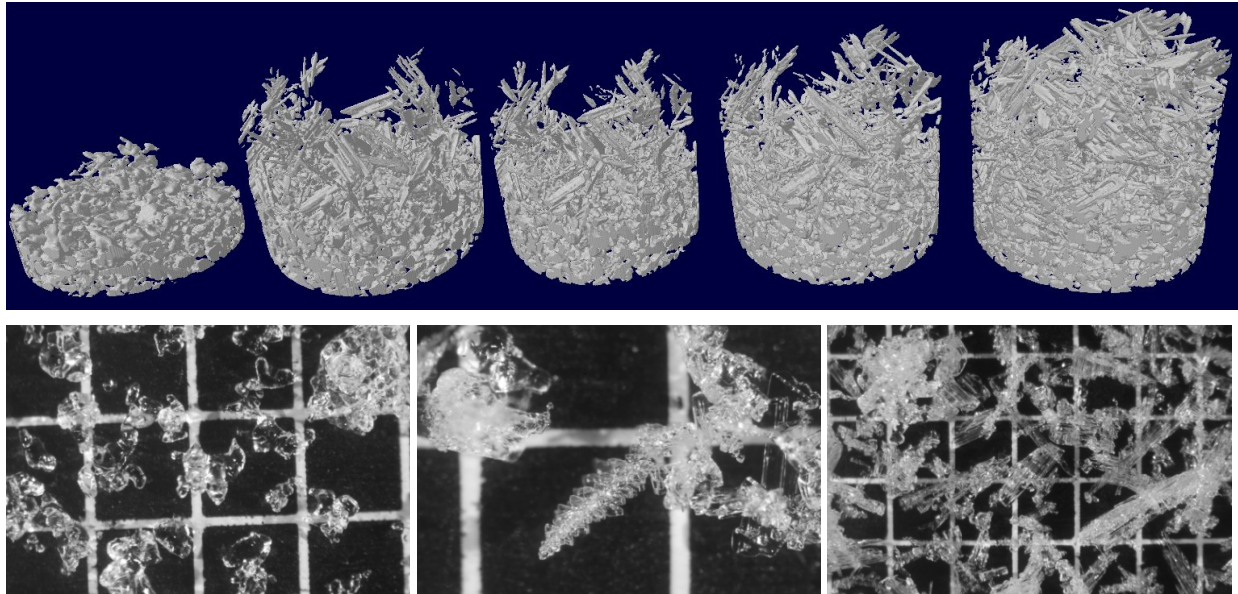


Figure 9: Test 2c. Snow Surface Temperature Range: -5.5 to -12.7°C. Mean Snow Surface Temperature: -8.3°C with a Standard Deviation of 0.76°C. CT Images at times: 0, 7, 11, 13.5, 23.5 (hrs) and (Sample Diameter: 8.4 mm) select microscopic images (2 mm grid) at times 0, 11, 23.5 (hrs).

Table 1: CT Data: Specific Surface Area (SSA). Scan 0 represents the SSA of the rounded grains before surface hoar growth. The remaining scans represent the SSA of only the deposited surface hoar. The tests 0-4 correspond to the CT images (left to right) in Figures 4-9.

Test	SSA (mm ⁻¹) 0	SSA (mm ⁻¹) 1	SSA (mm ⁻¹) 2	SSA (mm ⁻¹) 3	SSA (mm ⁻¹) 4	Mean Snow Surface Temp (°C)	Dominant Growth Axis
Test 1a	16.4	61.3	41.0			-29.9**	C
Test 1b	15.4	18.8	24.7			-15.5	A
Test 1c	18.6	54.1	43.4			-8.3	C
Test 2a	15.3	11.5	14.9	17.8	64.5	-29.7*	C
Test 2b	15.6	13.4	14.4	15.6		-15.0	A
Test 2c	13.2	22.3	19.7	17.7	20.9	-8.3	C

*During periods of actual surface hoar growth the snow surface temperature for the two stated tests was approximately -31°C.

**Data from first 7 hours only.

4. DISCUSSION

By controlling the air temperature, wind speed, humidity and long wave radiation exchange, surface hoar was consistently produced in a lab setting. The approach simulated the natural processes believed to be dominant in surface hoar development. Consistent with Kobayashi (1961), the surface hoar grown in this study displayed c-axis dominant growth in tests 1a and 2a where snow surface temperatures, during growth, were approximately -31°C as well as in tests 1c and 2c where average snow surface temperatures were approximately -8°C. The needle like form consistent with c-axis growth can be plainly seen in the final images in Figures 4, 6, 7, and 9. Likewise, crystals grown in tests 1b and 2b, at average surface temperatures of

approximately -15°C, demonstrated a-axis dominant growth. These cupped and feathery crystals can be seen in Figure 5 and 8. These results provide further confirmation that primary crystal habit temperature dependence of atmospheric snow crystals applies to surface hoar.

Table 1 also displays specific surface area (SSA) data. SSA is the ratio of the surface area of the ice to the total volume of the ice. Ice volume and surface area were obtained from the CT images using the SkyScan software.

For crystals displaying c-axis dominant growth, the initial surface hoar SSA (1) is much greater than for the rounded base snow (0). As surface hoar growth progressed and the crystals

became larger, there was a marked decrease in SSA. The exception to the trend of decreasing SSA in c-axis dominant growth is test 2a. It is speculated from relative humidity data that during the first 12.5 hours of this experiment conditions were not favorable to growth. This was verified, as the growth did not become evident until the later part of the test. Further, CT images (Figure 7) show very little change in the first 12.5 hours. Significant growth in test 2a only occurs in the final 12.5 hours. Had growth begun immediately at the start of the experiment it is expected that test 2a would also have shown a marked increase in SSA followed by decline. Conversely, in tests 1b and 2b, where a-axis growth dominated, the general trend tends to be toward increasing SSA with increasing surface hoar size.

The trend of decreasing SSA for c-axis growth and increasing SSA for a-axis growth is interesting and is likely attributed to the resulting crystal shapes. A-axis growth results in large plate like crystals, which have a correspondingly high SSA. Conversely, c-axis growth resulted in needle like crystals that have low SSA. The exception observed here is test 2a where significant growth was not observed until very late in the test, making the early SSA measurements not applicable.

5. CONCLUSIONS

Central to the natural growth of surface hoar is the cooling of the snow's surface due to long wave energy loss on clear nights. In this study, a methodology for realistically simulating this process was developed in a lab setting. Surface hoar was grown using a temperature controlled cold ceiling to simulate the cold sky. During growth periods, the snow surface temperature averaged $\sim 2\text{-}4^\circ\text{C}$ less than the ambient environmental chamber air temperature, creating the required temperature gradient for vapor deposition and the growth of surface hoar. Protocols for measuring air and snow surface temperature, long and short wave energy balance, and vertical temperature profile in the snow pack were established. The onset and growth of surface hoar on an existing snow surface was consistently demonstrated.

In addition, the time history of surface hoar growth at three different snow surface

temperatures was documented using both CT and optical microscopic imagery. The results show the three-dimensional development over time of needle like crystals at snow surface temperatures of -8°C and -29°C and the development of large feathery crystals at -15°C . These results are consistent with studies of crystal habits grown using fiber as a nucleation point. Finally, CT data allowed the tracking of SSA during surface hoar growth.

Further study will continue earlier work showing that the preferred axis of growth for surface hoar is affected by the crystallographic orientation of the parent grain on which the crystal is nucleating (Adams et. al., 2003). Additional work will attempt to predict final crystal habit, SSA, and growth rates of surface hoar based on recorded weather data. Additionally, the techniques reported here could be used in other studies examining bulk properties, strength, fracture properties, or optical properties of surface hoar.

5. ACKNOWLEDGEMENTS

The support provided by NSF Award Number 1014497 was greatly appreciated.

6. WORKS CITED

- Adams, E. and Miller, D., 2003. Ice crystals grown from vapor onto an orientated substrate: application to snow depth-hoar development and gas inclusions in lake ice. *Journal of Glaciology*, Vol. 49, 8-12.
- Hallet, J. and Mason, B.J., 1958. The influence of temperature and supersaturation on the habit of ice crystals growth from the vapor. *Proc. Roy. Soc. Lond*, A(247), 440-453.
- Kobayashi, T., 1961. The growth of snow crystals at low supersaturation. *Phil. Mag.* 6, 1363—1370.
- Lang, R., Leo, B., and Brown, R., 1984. Observations on the growth process and strength characteristics of surface hoar. In *International Snow Science Workshop*, Aspen, CO.
- Nakaya, U., 1954. Snow crystals: natural and artificial. Harvard Univ. Press, Cambridge, Mass.